

Measurement of mixed-mode *cohesive laws* of a UD composite undergoing delamination with large-scale fibre bridging

Ruben Erives

Supervisor: Bent Sørensen

Overview



Motivation



Derivation of cohesive law



Experimental Characterisation



Results



Concluding remarks



Questions & discussion

Why is it important to measure cohesive tractions?

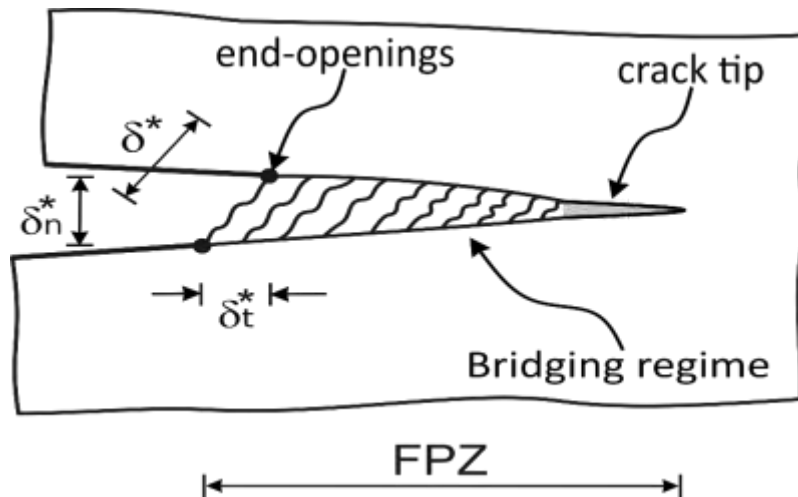
1. A material/interface property should be measurable. Ideally we'd like to first measure a property first, and then use it on a model, not the other way around.
2. Idealised cohesive laws have a number of shortcomings
 1. The traction separation law is fully determined by the combined work of the peak traction and a critical opening. Then the shape (and peak traction) are predefined
 2. Difficult or not possible to recover R-curves from pre-defined cohesive laws
3. The shape of the cohesive traction conveys important information of the fracture behaviour of a material e.g., crack stability
4. When measuring cohesive tractions from R-curves there is no need to impose any mixed-mode criterion

Derivation of cohesive law

Definition of end-openings and phase angle

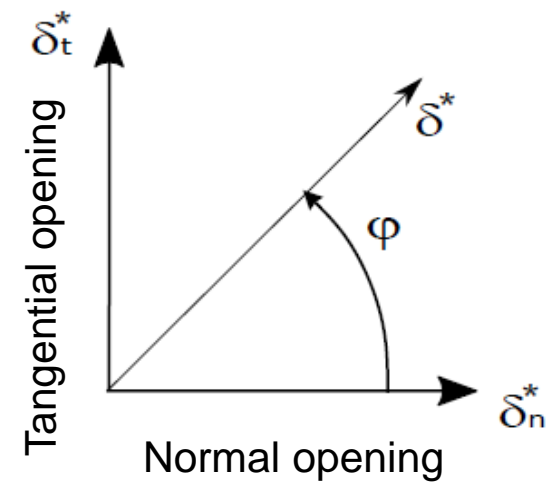
End-opening

$$\delta^* = \sqrt{\delta_n^* + \delta_t^*}$$



Phase angle

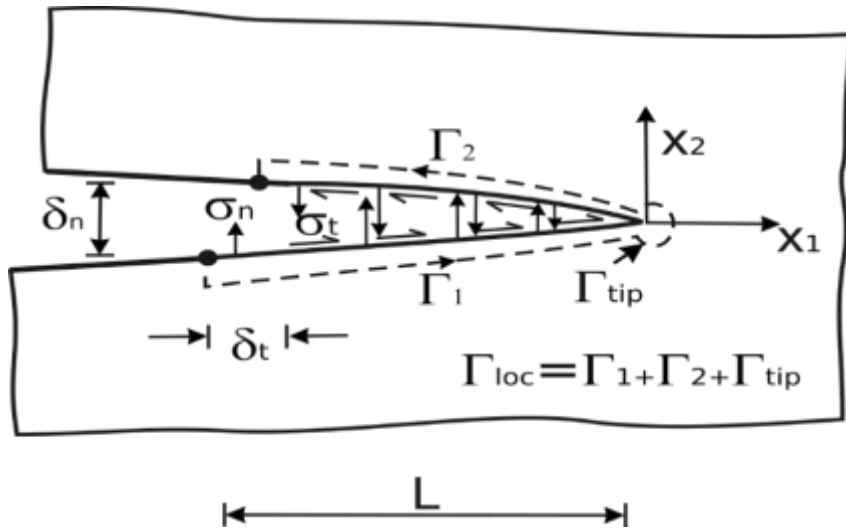
$$\varphi^* = \tan^{-1} \left(\frac{\delta_t^*}{\delta_n^*} \right)$$



DTU Derivation of cohesive law

J-integral approach

Applying the J-integral around Γ_{loc} results in



Assuming that the cohesive tractions can be derived from a potential function, Φ , then

Path-independent $\longrightarrow \Phi = \Phi(\delta_n, \delta_t)$

$$\Phi(0,0) = 0$$

So that,

Mixed mode coupled cohesive tractions

$$J_{loc} = \int_0^{\delta_n^*} \sigma_n(\delta_n, \delta_t) d\delta_n + \int_0^{\delta_t^*} \sigma_t(\delta_n, \delta_t) d\delta_t$$

[Sørensen and Kirkegaard, 2006]

Relates Φ to R-curves $\longrightarrow J_R = J_{loc} = \Phi(\delta_n^*, \delta_t^*)$

Cartesian

$$\sigma_n(\delta_n, \delta_t) = \frac{\partial \Phi(\delta_n, \delta_t)}{\partial \delta_n}$$

$$\sigma_t(\delta_n, \delta_t) = \frac{\partial \Phi(\delta_n, \delta_t)}{\partial \delta_t}$$

Cylindrical

$$\sigma_n(\delta, \varphi) = \cos(\varphi) \frac{\partial \Phi}{\partial \delta} - \frac{\sin(\varphi)}{\delta} \frac{\partial \Phi}{\partial \varphi}$$

$$\sigma_t(\delta, \varphi) = \sin(\varphi) \frac{\partial \Phi}{\partial \delta} + \frac{\cos(\varphi)}{\delta} \frac{\partial \Phi}{\partial \varphi}$$

DTU Derivation of cohesive law

Piece-wise, cylindrical potential function

- The potential function is defined in a piece-wise function:

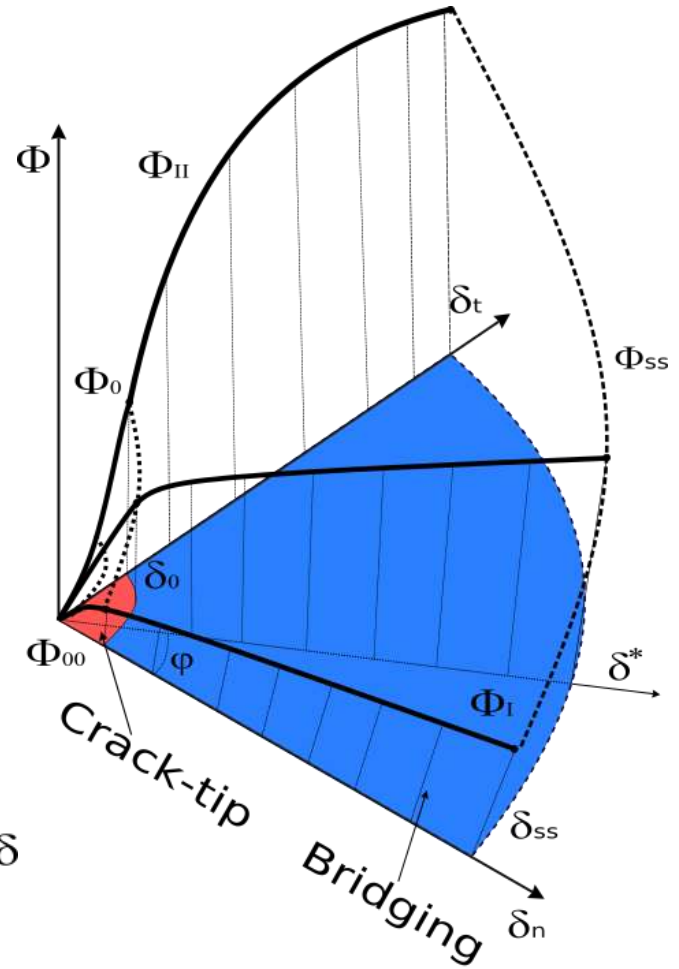
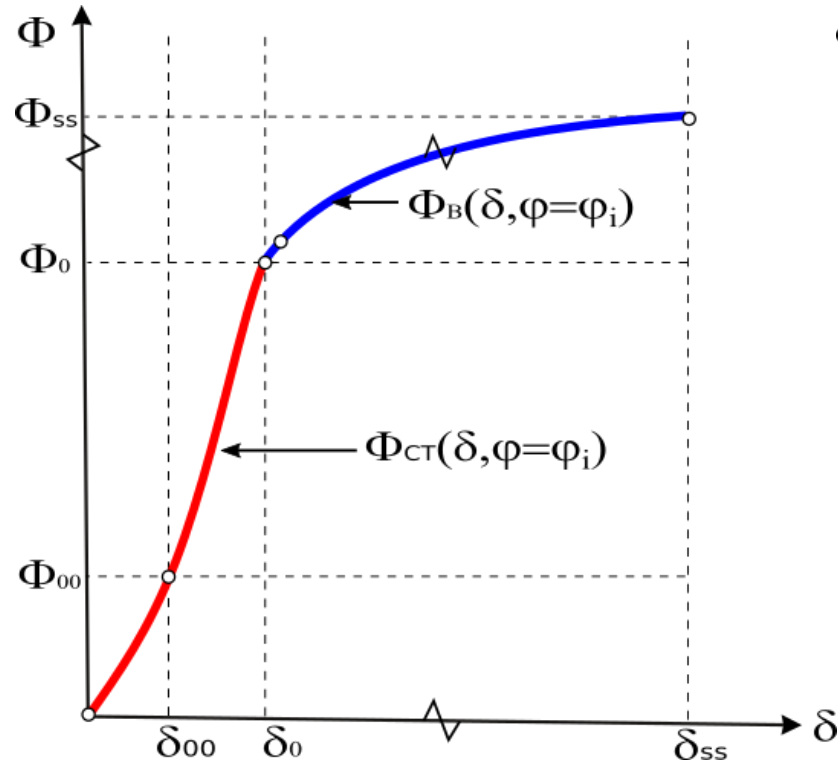
$$\Phi(\delta, \varphi) = \begin{cases} \Phi_{CT}, & 0 < \delta^* \leq \delta_0 \\ \Phi_B, & \delta_0 < \delta^* \leq \delta_{ss} \end{cases}$$

$$\Phi_{CT}(\delta^*, \varphi^*) = C_3 \delta^{*3} + C_2 \delta^{*2} + C_1 \delta^* + C_0$$

$$\Phi_B(\delta^*, \varphi^*) = \Phi_0 + (\Phi_{ss} - \Phi_0) \left(\frac{\delta^* - \delta_0}{\delta_{ss}} \right)^\zeta$$

- Parameters:

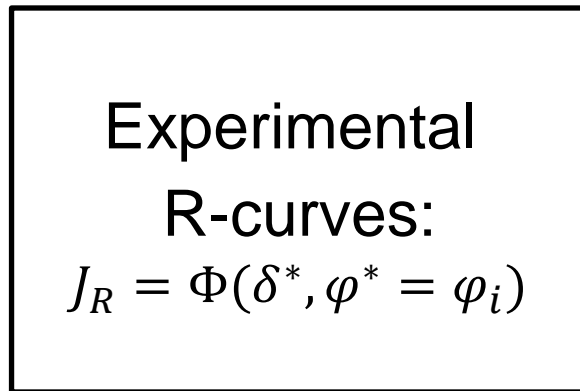
$$\Phi_0, \Phi_{ss}, \delta_0, \delta_{ss}, \zeta, \delta_{00}, \Phi_{00}$$



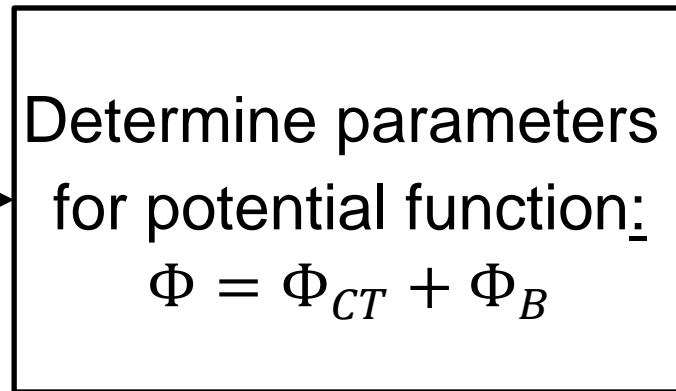
Experimental Characterisation

General procedure

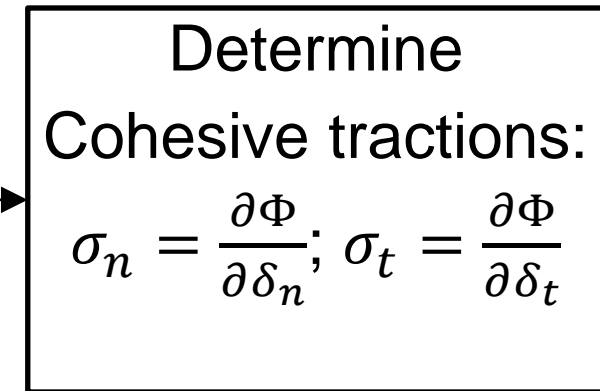
Step 1



Step 2



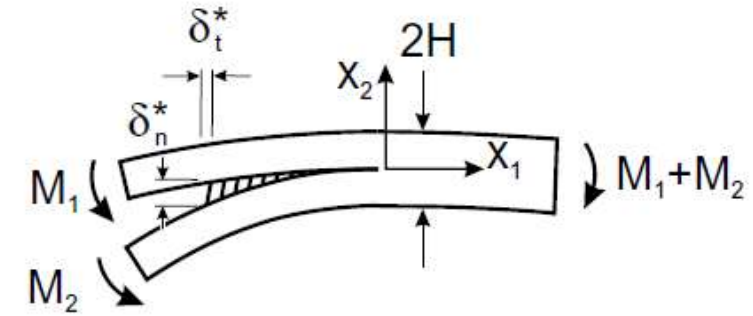
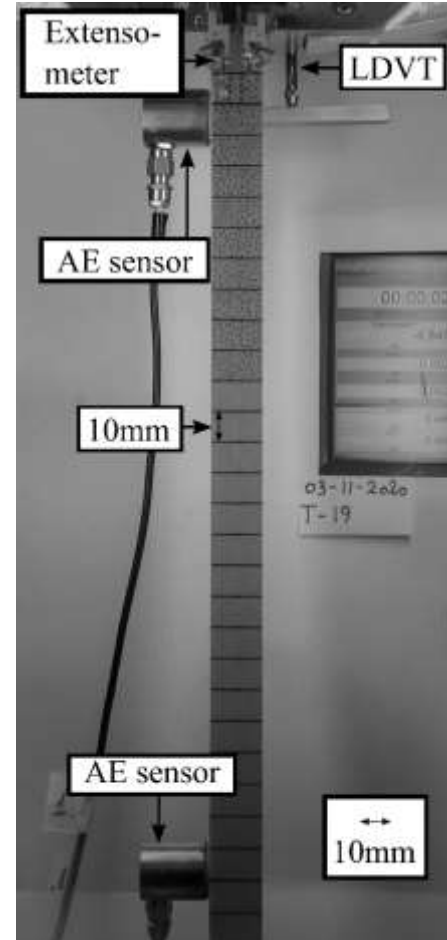
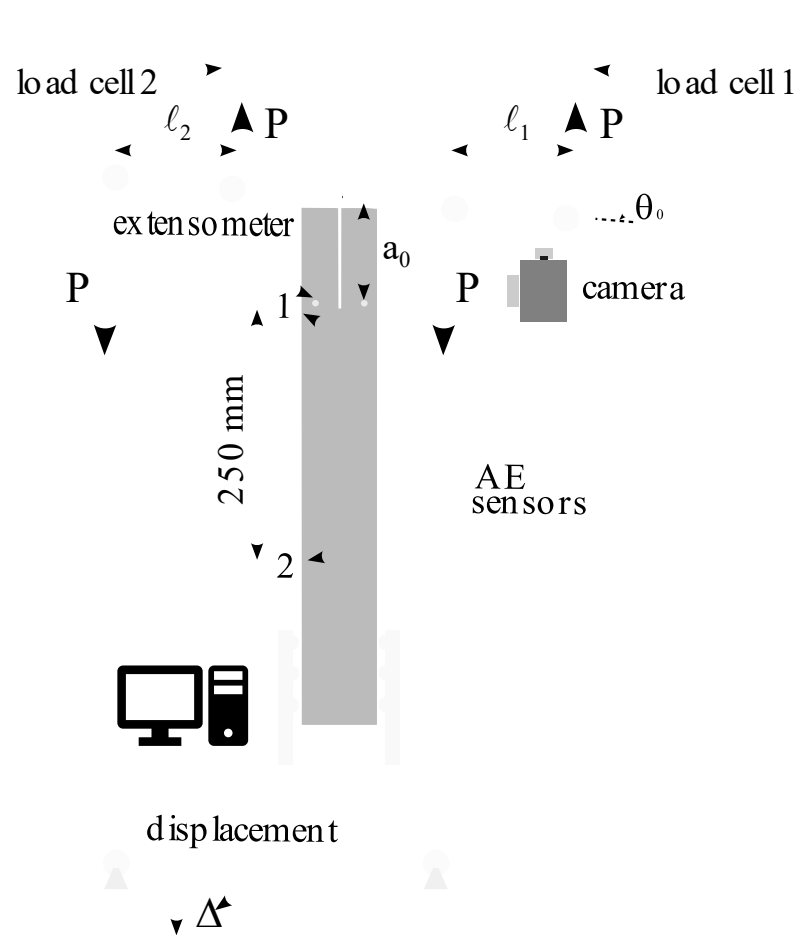
Step 3



Experimental characterisation

Double cantilever beam under uneven bending moments DCB-UBM

Test set-up



J-integral:

$$J_R = \frac{21(M_1^2 + M_2^2) - 6M_1M_2}{4B^2H^3E^*}$$

Experimental characterisation

Specimens and test groups

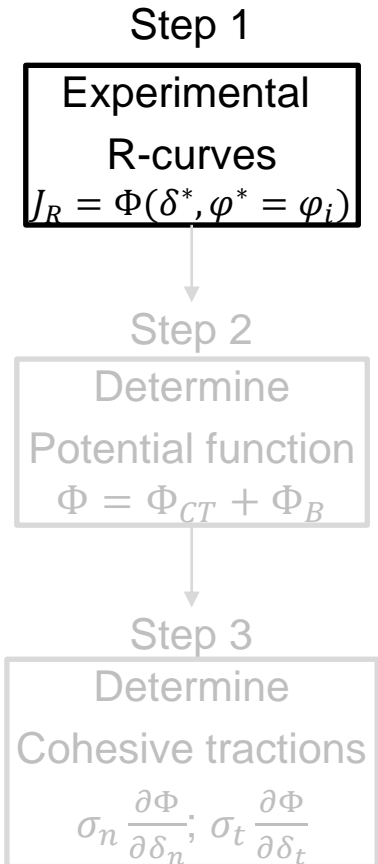


Table 1: List of different mixed-mode tests

Group	M_1/M_2 [-]	φ^* [Deg.]
1	-1.00	0.00 +/- 0.0
2	-0.66	2.72 +/- 1.1
3	-0.41	4.88 +/- 0.7
4	0.00	8.82 +/- 3.0
5	0.12	9.90 +/- 0.1
6	0.50	23.46 +/- 2.8
7	0.805	43.46 +/- 13.1
8	0.87	51.59 +/- 2.4
9a,b	0.87	50.62 +/- 5.2
10 ^b	0.96	64.95 +/- 2.8
11 ^b	0.99	67.88 +/- 4.8

a, the same moment ratio was tested twice in order to obtain steady-state

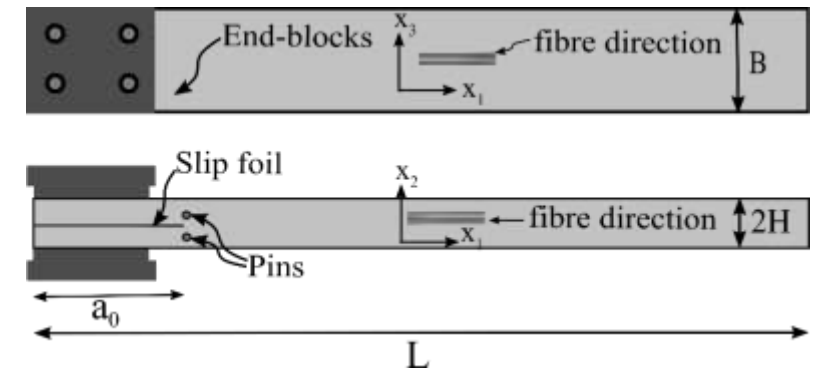
b, Tests carried out after submission of thesis. It was suggested during internal review of paper B

Table 2: Elastic properties of UD glass/epoxy laminate (Antoniou et al 2020)

Prop.	value	Unit
E_1	46.3	GPa
ν_{12}	0.26	-
E_2	12.92	GPa
G_{12}	4.3	GPa

Table 3: Geometric properties of standard DCB specimen

Prop.	value	Unit
a_0	70	mm
L	500	mm
B	30	mm
$2H$	20	layers
	~17	mm



DTU Experimental characterisation

Extraction of parameters

Step 1

R-curves

J_R

Step 2

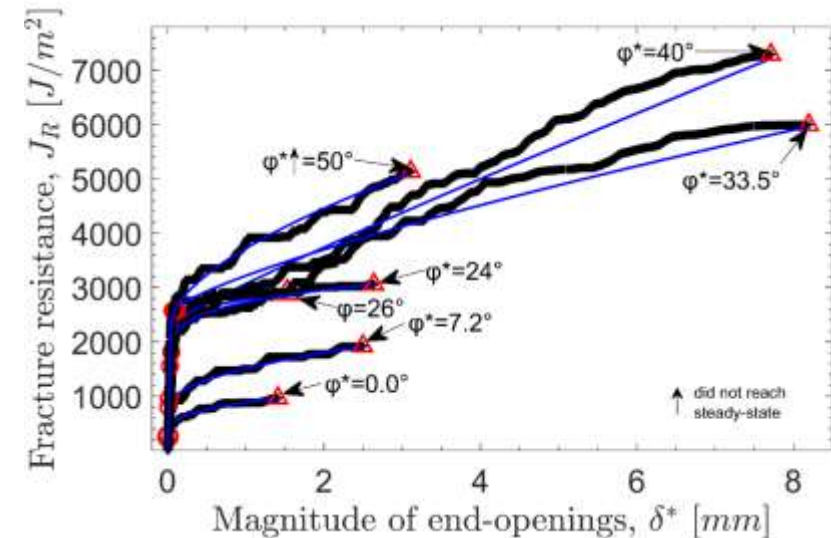
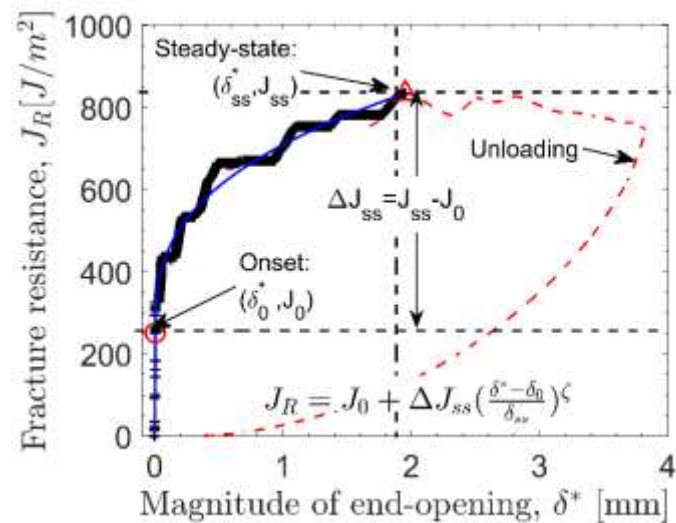
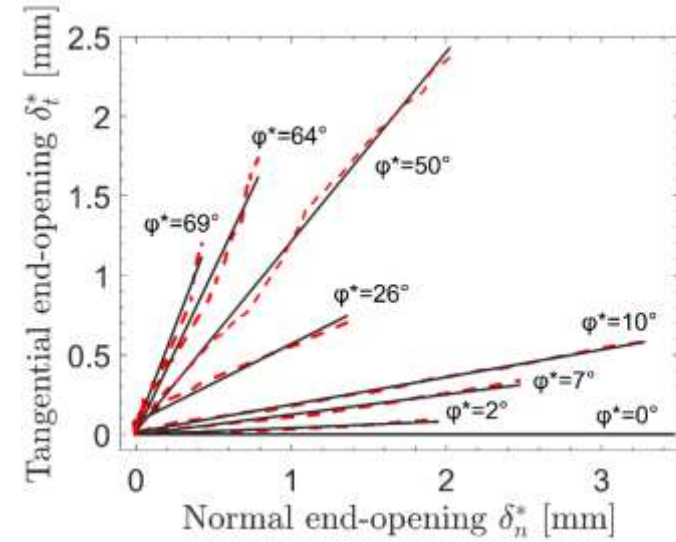
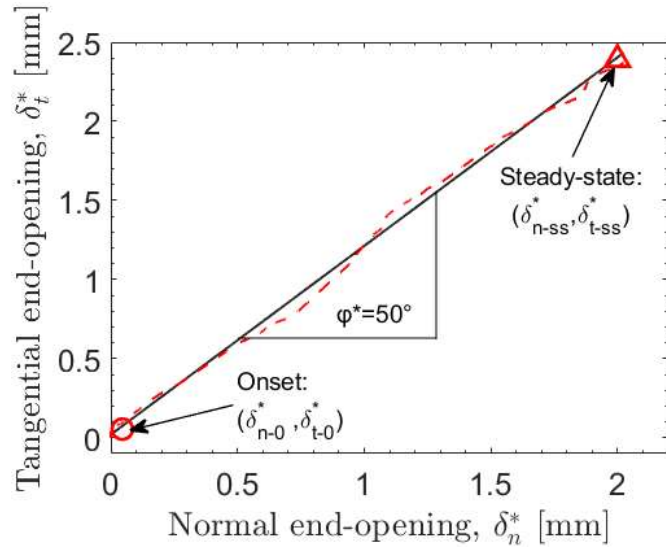
Potential function

$$\Phi = \Phi_{CT} + \Phi_B$$

Step 3

Cohesive tractions

$$\sigma_n \frac{\partial \Phi}{\partial \delta_n}; \sigma_t \frac{\partial \Phi}{\partial \delta_t}$$



DTU Experimental characterisation

Interpolation of parameter

Step 1

R-curves

$$J_R$$

Step 2

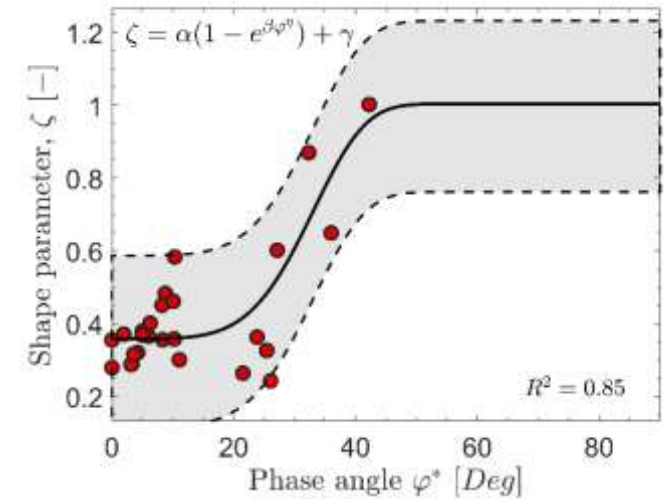
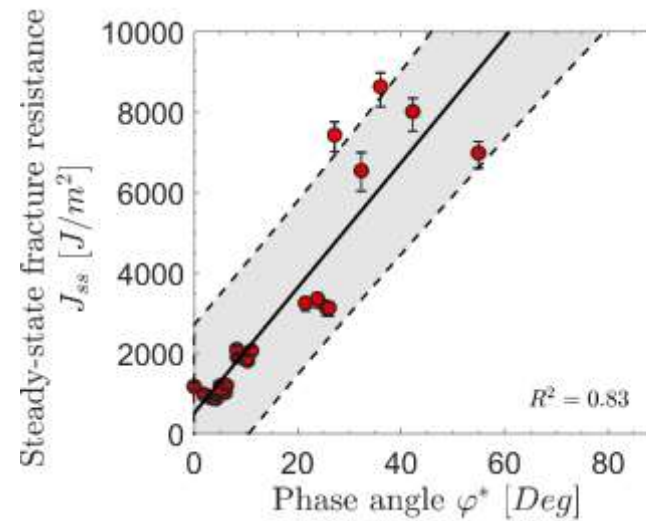
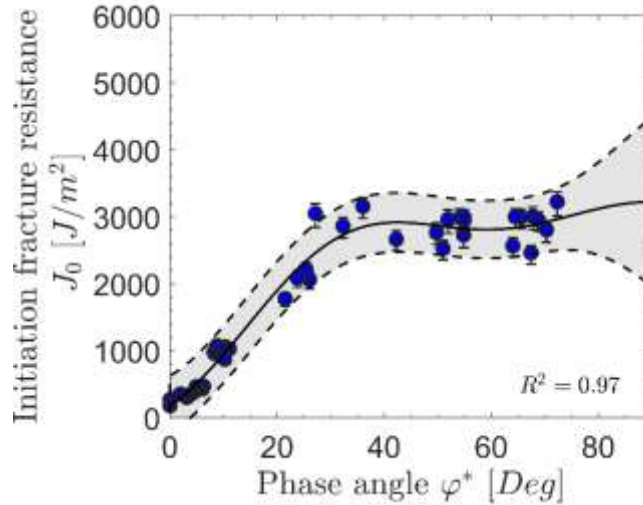
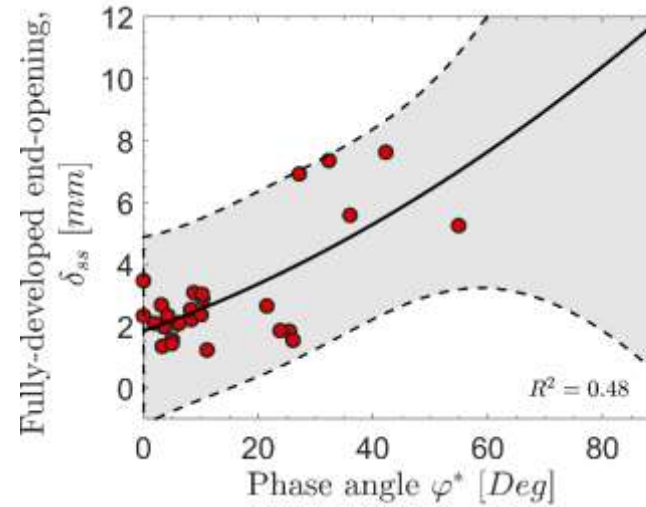
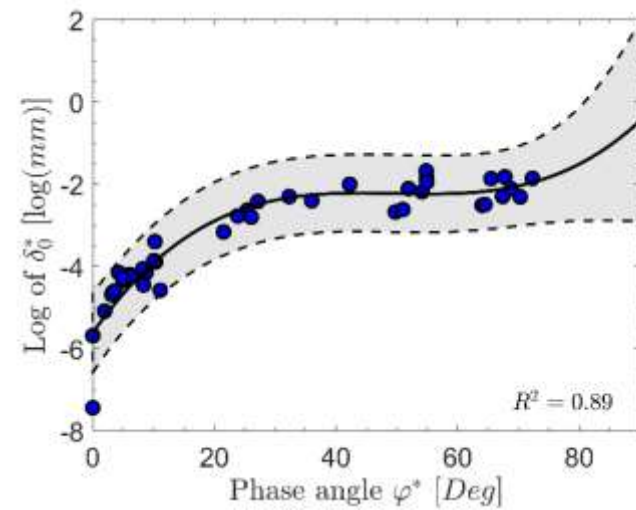
Potential function

$$\Phi = \Phi_{CT} + \Phi_B$$

Step 3

Cohesive tractions

$$\sigma_n \frac{\partial \Phi}{\partial \delta_n}; \sigma_t \frac{\partial \Phi}{\partial \delta_t}$$



DTU Experimental characterisation

Fitting of fracture resistance

Step 1

R-curves

J_R

Step 2

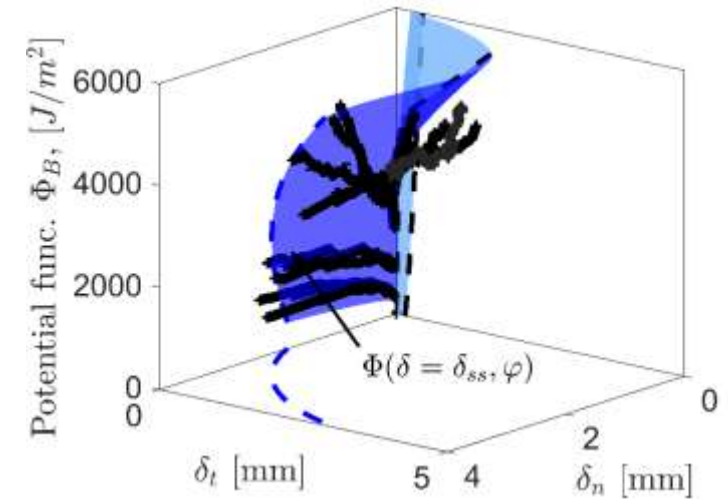
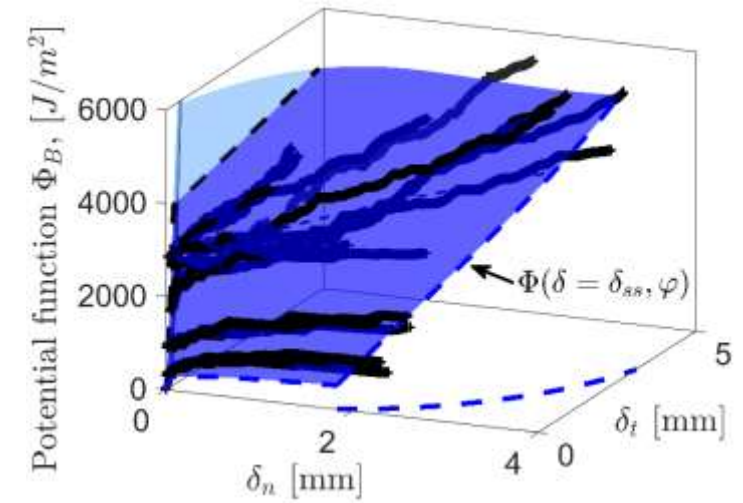
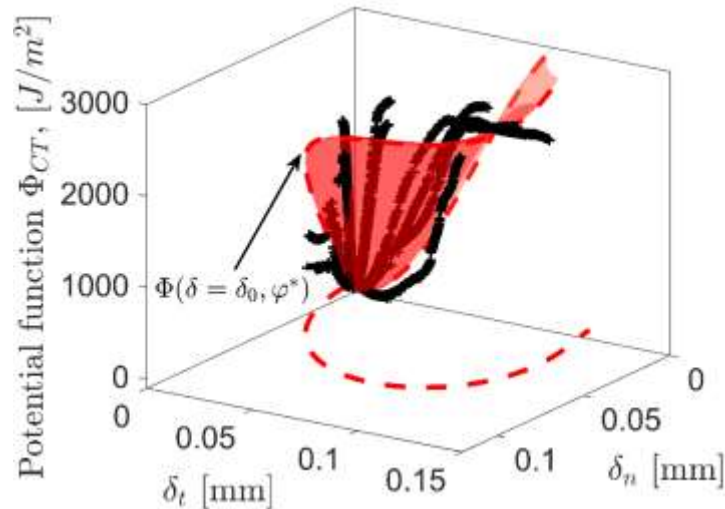
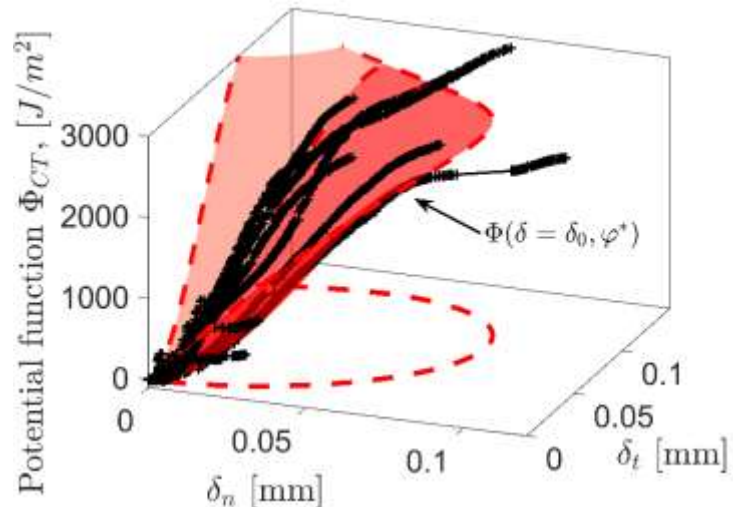
Potential function

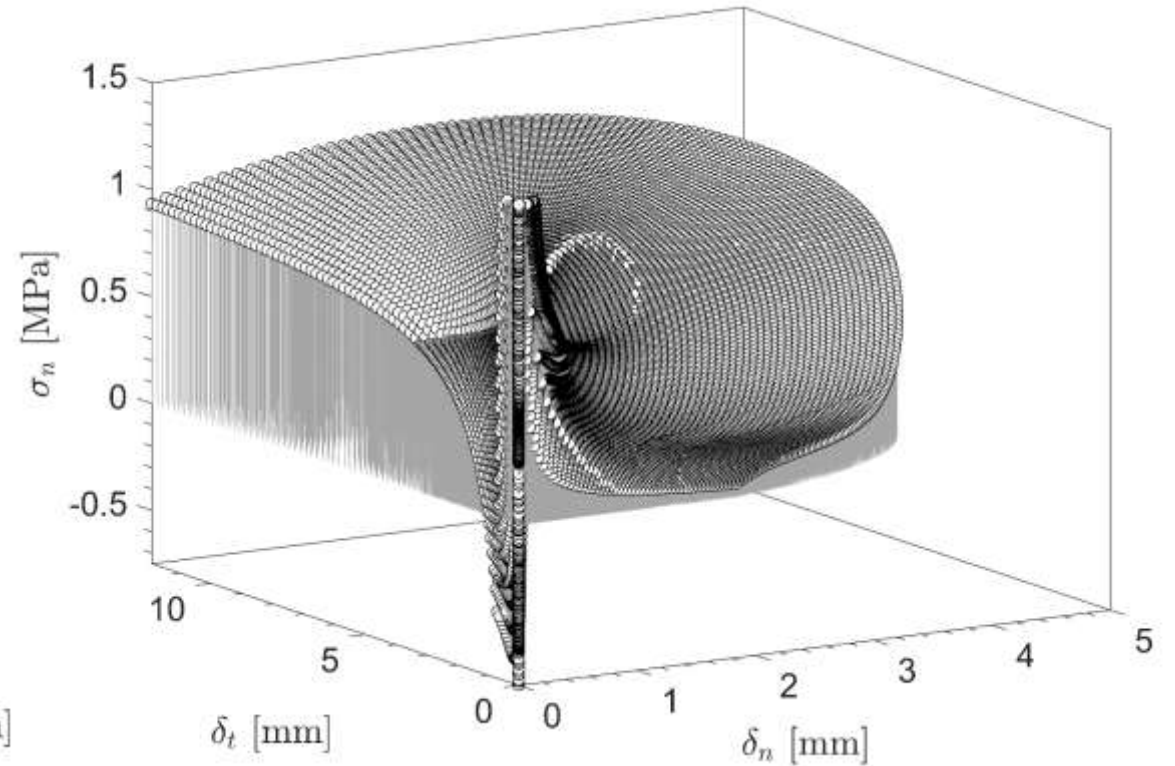
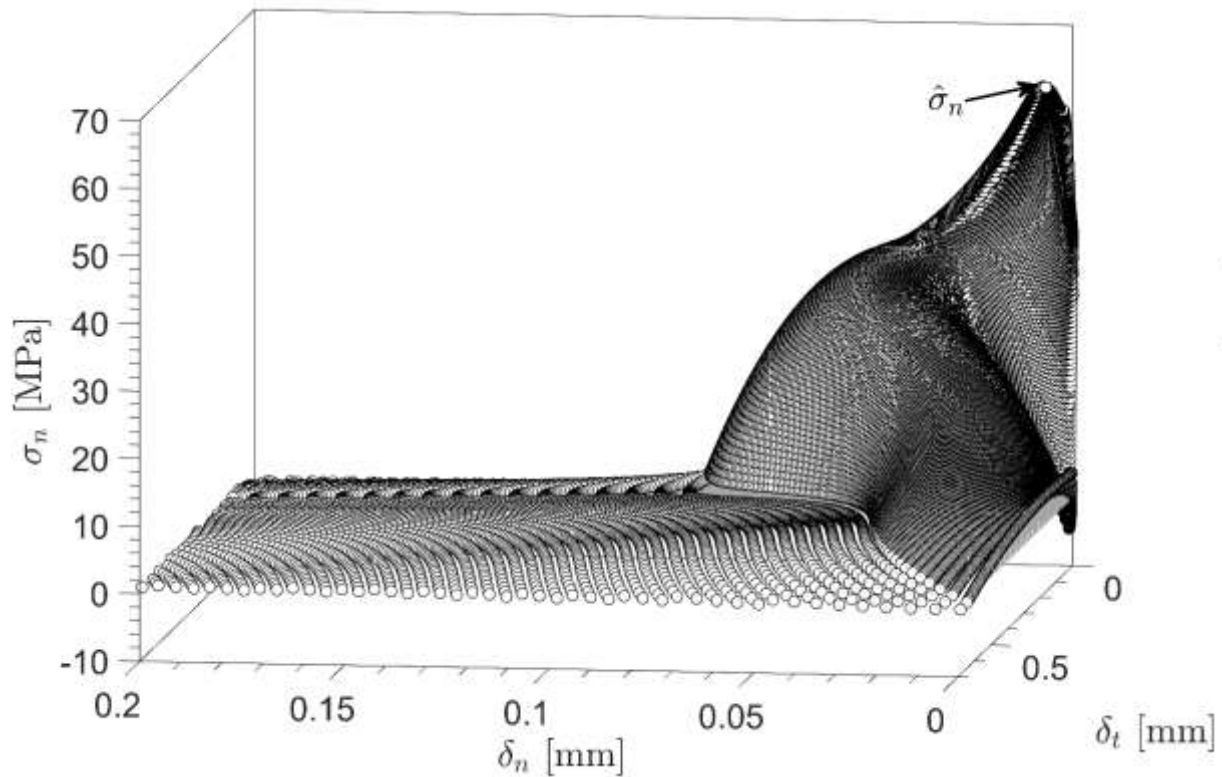
$$\Phi = \Phi_{CT} + \Phi_B$$

Step 3

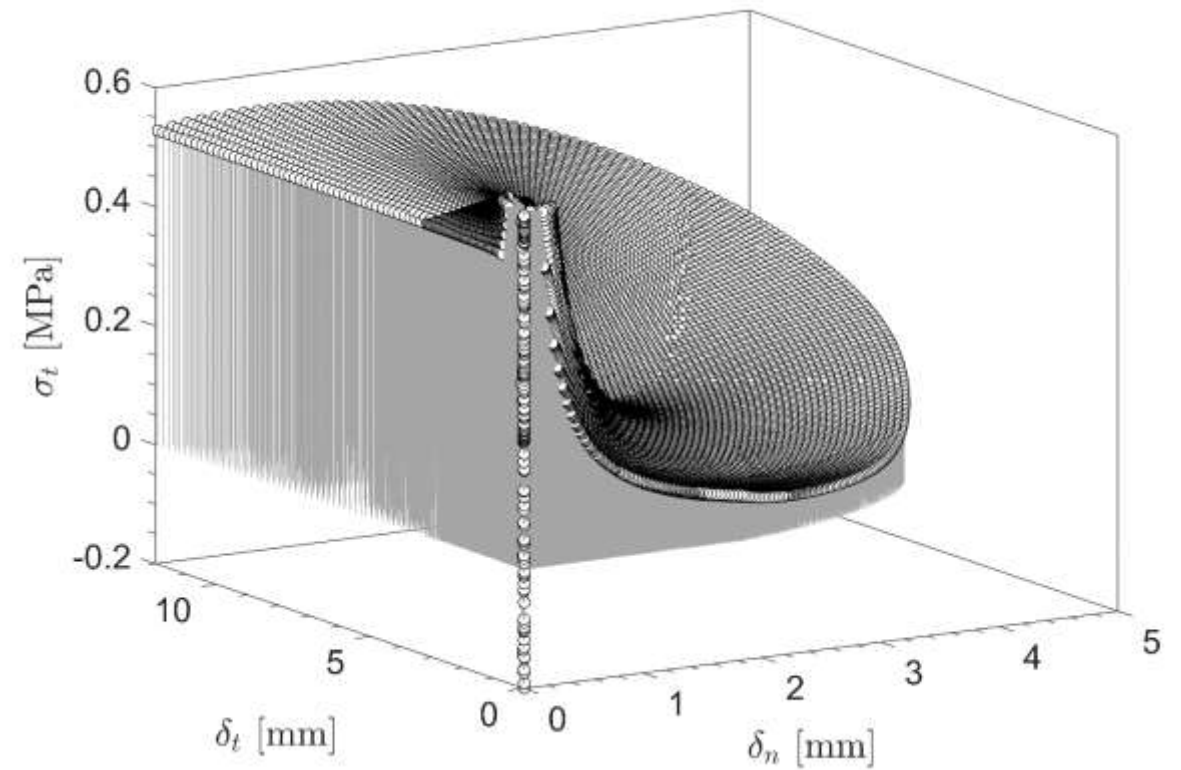
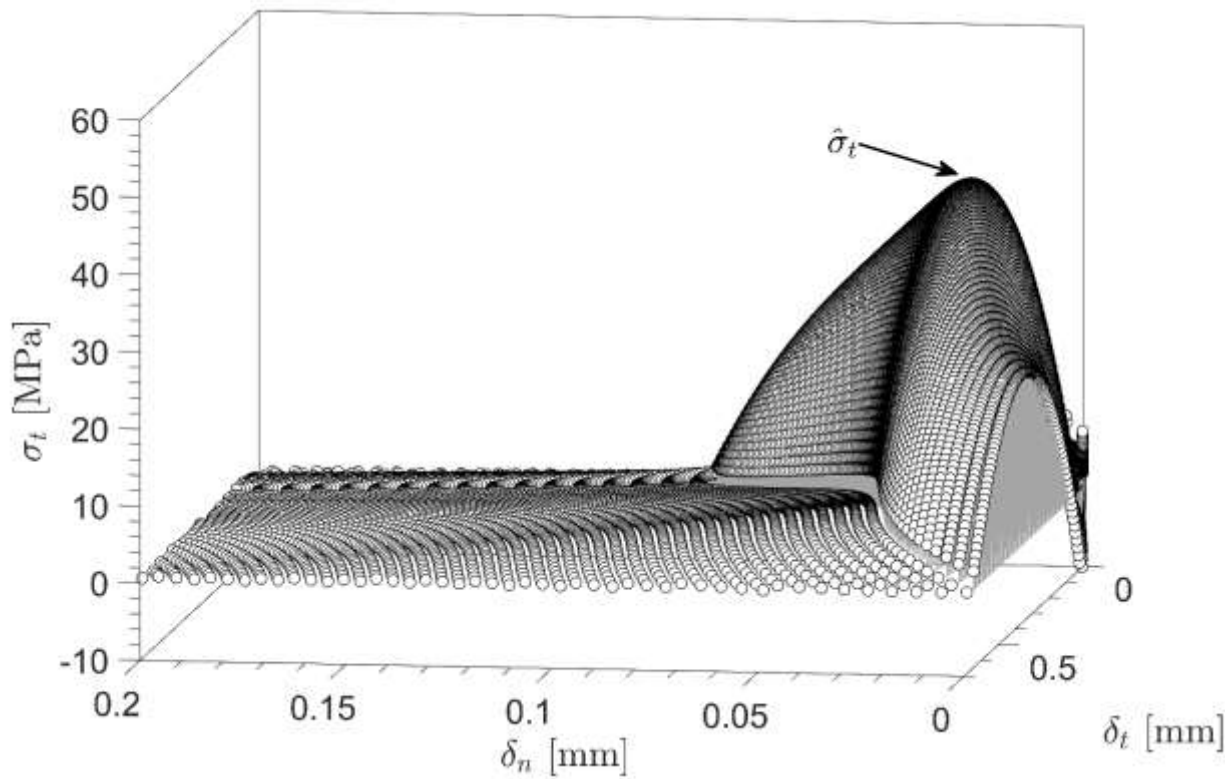
Cohesive tractions

$$\sigma_n \frac{\partial \Phi}{\partial \delta_n}; \sigma_t \frac{\partial \Phi}{\partial \delta_t}$$



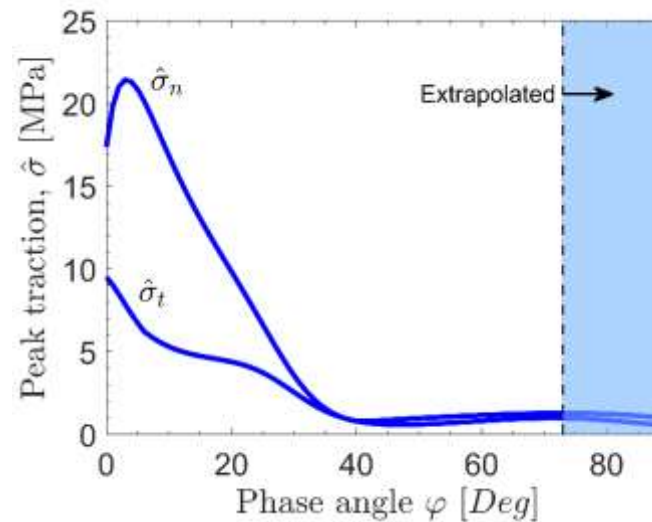
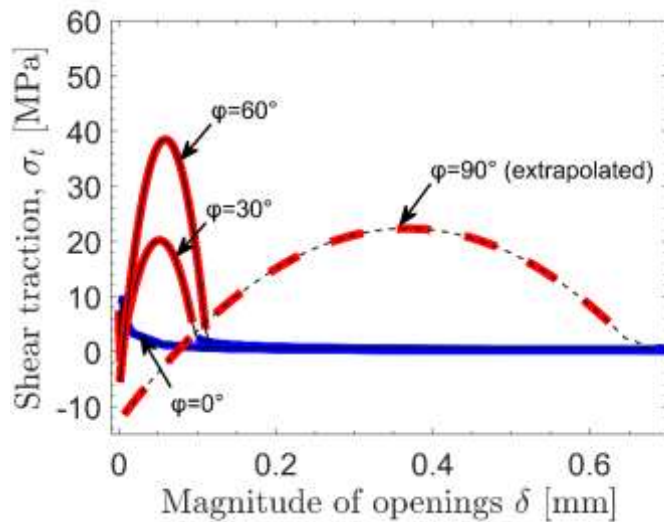
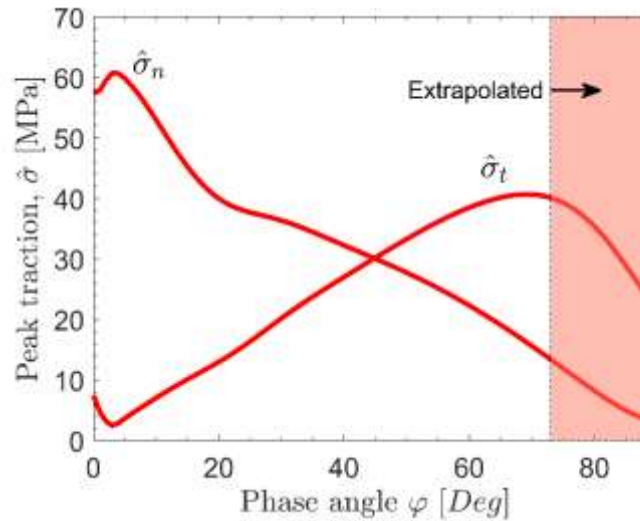
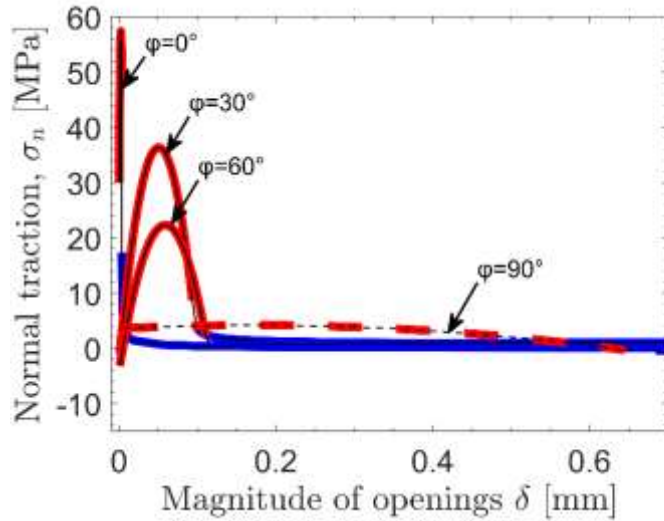


Non-zero normal traction for $\delta_n = 0$
 Negative normal traction for large φ



Non-zero shear traction for $\delta_t = 0$

Cohesive tractions – Peak tractions



Concluding remarks

1. The approach enables separate cohesive laws for the crack-tip (high traction values $\approx 30\text{--}60\text{MPa}$, small separations $\approx 10\text{--}100\ \mu\text{m}$) and bridging (low traction values $\approx 10\text{MPa}$, large separations $\approx 3\text{--}8\text{mm}$). Such a description is more realistic than the state-of-the-art idealised cohesive laws.
2. The measured cohesive laws are fully coupled (both normal and shear). Non-zero shear tractions are found for pure normal openings, and non-zero normal tractions are found
3. The surfaces of the normal and shear tractions have distinctively different shapes.
4. Non-monotonic variation of J_0 as a function of the phase angle, φ has been observed



Questions & Discussion

Backup slides

DTU



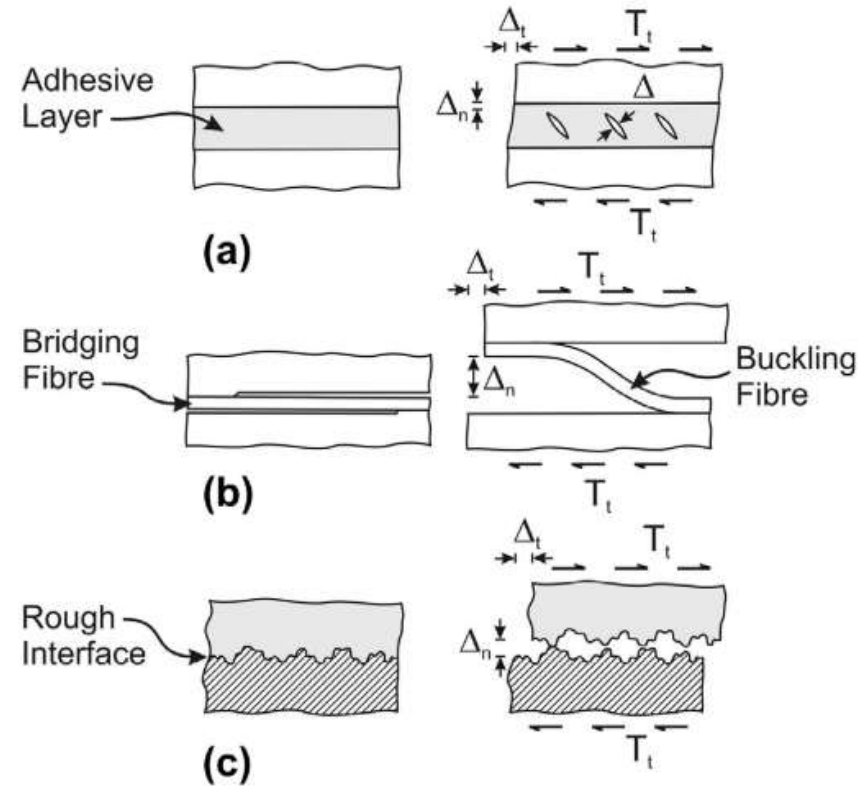
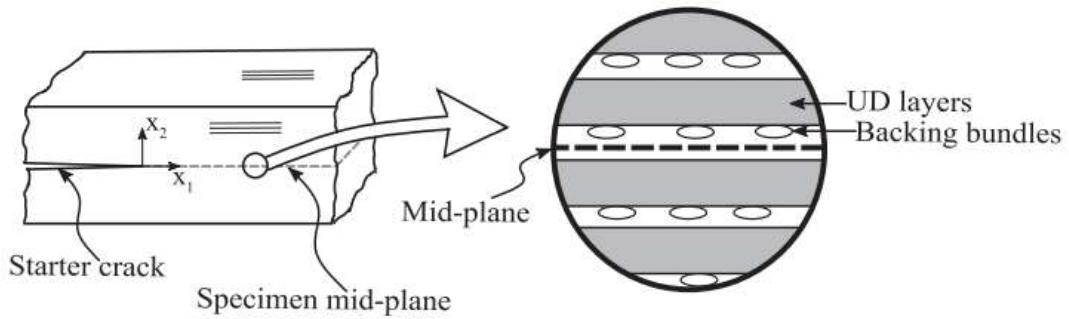


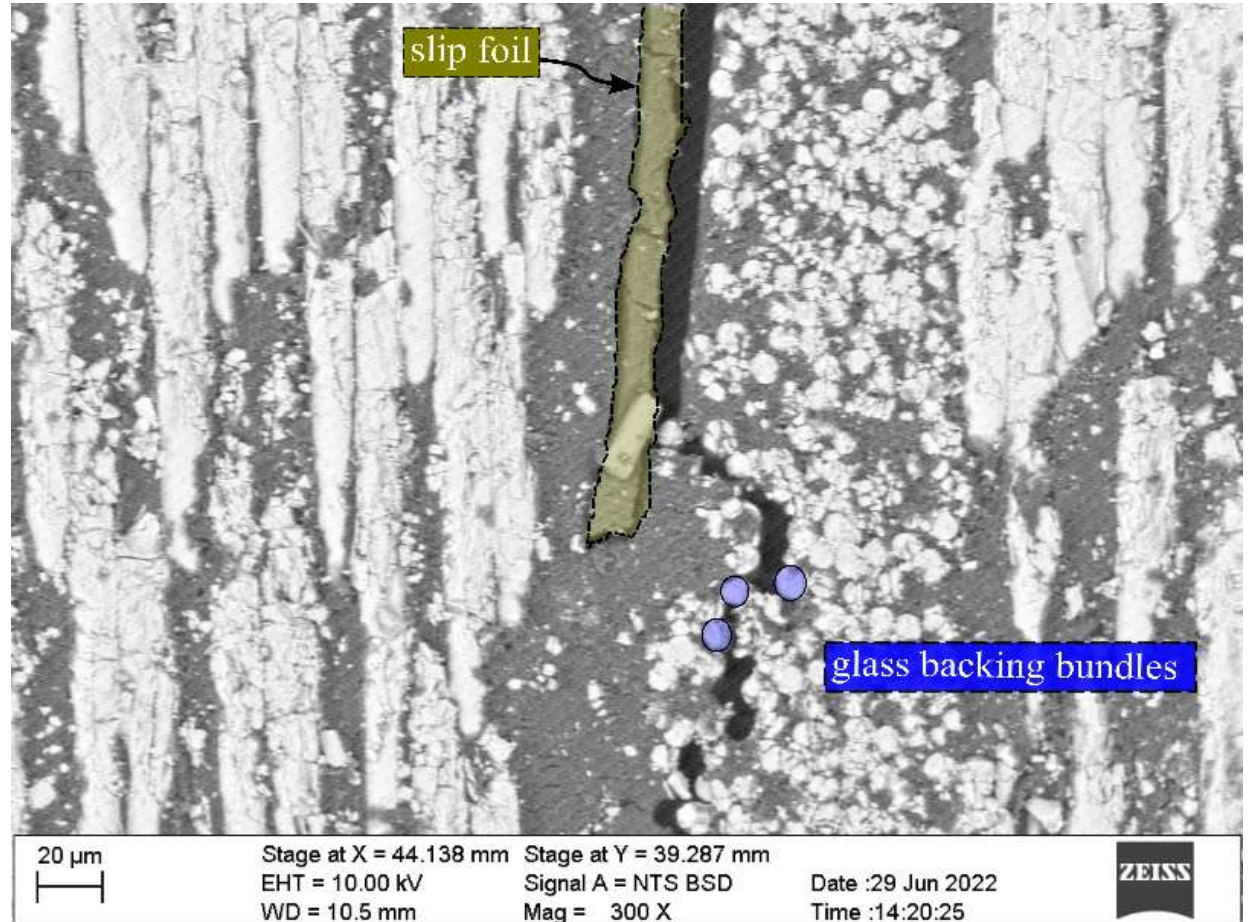
Fig. 1. Mechanisms that induced **interface dilatation** (normal opening during imposed tangential displacement): (a) shear cracks, (b) bridging fibres connecting the crack faces in such a manner that they buckle in compression, and (c) interface roughness.

Sørensen, B. F., & Goutianos, S. (2014). Mixed Mode cohesive law with interface dilatation. *Mechanics of Materials*, 70, 76–93.

Assymetric interface



Erives, R. 2023



20 μ m

Stage at X = 44.138 mm
EHT = 10.00 kV
WD = 10.5 mm

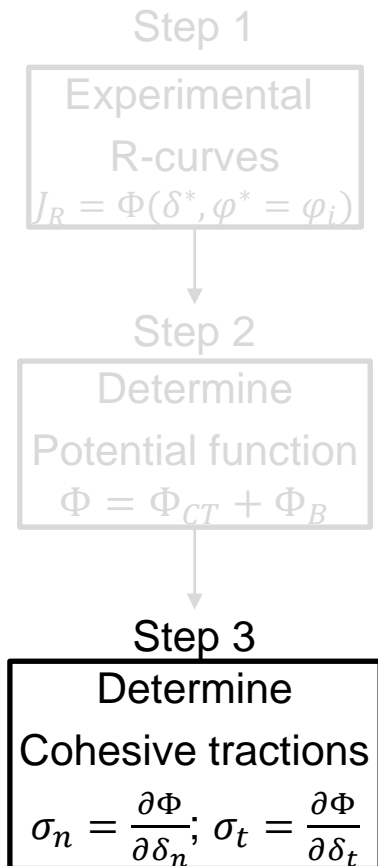
Stage at Y = 39.287 mm
Signal A = NTS BSD
Mag = 300 X

Date :29 Jun 2022
Time :14:20:25



Experimental characterisation

Determination of cohesive tractions by partial differentiation



$$\frac{\partial \Phi}{\partial \delta^*} = \begin{cases} 3C_3(\varphi)\delta^{*2} + 2C_2(\varphi)\delta^* + C_1(\varphi), & 0 < \delta \leq \delta_0 \\ \frac{\Delta\Phi_{ss}}{\delta_{ss}} \zeta \left(\frac{\delta^* - \delta_0}{\delta_{ss}} \right)^{\zeta-1}, & \delta_0 < \delta \leq \delta_{ss} \end{cases}$$

$$\frac{\partial \Phi}{\partial \varphi} = \begin{cases} \frac{\partial C_3}{\partial \varphi} \delta^{*3} + \frac{\partial C_2}{\partial \varphi} \delta^{*2} + \frac{\partial C_1}{\partial \varphi} \delta^* + \frac{\partial C_0}{\partial \varphi}, & 0 < \delta \leq \delta_0 \\ \frac{\partial \Phi_0}{\partial \varphi} + \frac{\partial(\Delta\Phi_{ss})}{\partial \varphi} D + \Delta\Phi_{ss} \left(A \frac{\partial \delta_0}{\partial \varphi} + B \frac{\partial \delta_{ss}}{\partial \varphi} + C \frac{\partial \zeta}{\partial \varphi} \right), & \delta_0 < \delta \leq \delta_{ss} \end{cases}$$

$$\sigma_n(\delta^*, \varphi) = \cos(\varphi) \frac{\partial \Phi}{\partial \delta^*} - \frac{\sin(\varphi)}{\delta^*} \frac{\partial \Phi}{\partial \varphi}$$

$$\sigma_t(\delta^*, \varphi) = \sin(\varphi) \frac{\partial \Phi}{\partial \delta^*} + \frac{\cos(\varphi)}{\delta^*} \frac{\partial \Phi}{\partial \varphi}$$

$$A = -D\zeta \frac{1}{\delta^* - \delta_0}$$

$$B = -D \frac{\zeta}{\delta_{ss}}$$

$$C = -\ln \left\{ \frac{\delta^* - \delta_0}{\delta_{ss}} \right\} D$$

$$D = \left(\frac{\delta^* - \delta_0}{\delta_{ss}} \right)^\zeta$$

Criteria for stable growth

- For materials with an R-curve behaviour a criterion for stable crack growth is:

$$J_{Ext} = J_R \quad \text{and} \quad \frac{\partial J_{Ext}}{\partial \ell} \leq \frac{\partial J_R}{\partial \ell}$$

$$\frac{\partial J_{Ext}}{\partial \ell} \leq \frac{\partial \Phi(\delta_n, \delta_t)}{\partial \ell}$$

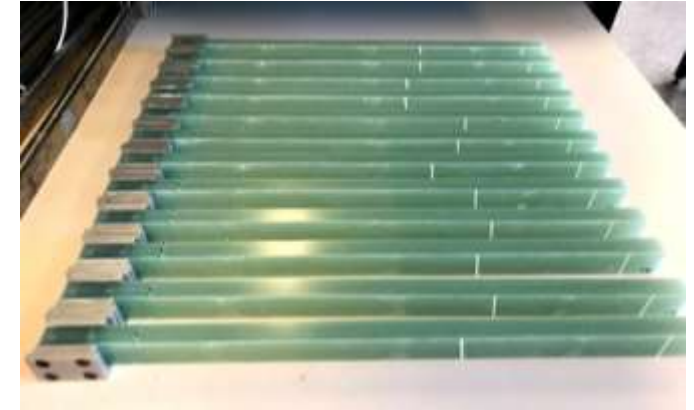
$$\frac{\partial \Phi(\delta_n, \delta_t)}{\partial \ell} = \frac{\partial \Phi(\delta_n, \delta_t)}{\partial \delta_n} \frac{\partial \delta_n}{\partial \ell} + \frac{\partial \Phi(\delta_n, \delta_t)}{\partial \delta_t} \frac{\partial \delta_t}{\partial \ell}$$

$$\frac{\partial \Phi(\delta_n, \delta_t)}{\partial \ell} = \sigma_n(\delta_n, \delta_t) \frac{\partial \delta_n}{\partial \ell} + \sigma_t(\delta_n, \delta_t) \frac{\partial \delta_t}{\partial \ell}$$

$$\text{Structure} \quad \frac{\partial J_{Ext}}{\partial \ell} \leq \underbrace{\sigma_n(\delta_n, \delta_t)}_{\text{Material}} \underbrace{\frac{\partial \delta_n}{\partial \ell}}_{\text{Structure}} + \underbrace{\sigma_t(\delta_n, \delta_t)}_{\text{Material}} \underbrace{\frac{\partial \delta_t}{\partial \ell}}_{\text{Structure}} \quad \text{Material}$$

1. Materials and Specimens

- Lay-up: 20 UD-layers (backing facing downwards on all layers – Not symmetrical)
- Fabric type: UD= E-E-1182 Saertex
- Matrix: Epoxy Hexion RIMR 035c / RIMH 037 100/28
- Curing procedure: 12h@40C+10h@80C
- VF of 55%



DCB specimens geometry

